Efficient Image Registration using Fast Principal Component Analysis

Conference or Workshop Item

EFFICIENT IMAGE REGISTRATION USING FAST PRINCIPAL COMPONENT ANALYSIS

Parminder Singh Reel, Laurence S Dooley and Patrick Wong
Department of Communication and Systems, The Open University, Milton Keynes, United Kingdom
Email: p.s.reel|l.s.dooley|k.c.p.wong@open.ac.uk

ABSTRACT

Incorporating spatial features with mutual information (MI) has demonstrated superior image registration performance compared with traditional MI-based methods, particularly in the presence of noise and intensity non-uniformities (INU). This paper presents a new efficient MI-based similarity measure which applies Expectation Maximisation for Principal Component Analysis (EMPCA-MI), to afford significantly lower computational complexity, while providing analogous image registration performance with other feature-based MI solutions. Experimental analysis corroborates both the improved robustness and faster runtimes of EMPCA-MI, for different test datasets containing both INU and noise artefacts.

Index Terms — Expectation maximisation algorithms, principal component analysis, mutual information, image registration.

1. INTRODUCTION

Image registration (IR) is a key processing step in many application domains, where the final information is obtained by combining different data sources, such as in medical imaging, remote sensing and computer vision [1]. It involves the geometric transformation of a source image so it attains physical alignment with a reference target image. Subsequently, an optimization is performed with known transformations to maximise a predefined similarity measure between the source and reference images.

Similarity measures which have been proposed [1] for IR, can be broadly classified according to whether they are based on cross-correlation, *mutual information* (MI) or Fourier techniques, with MI being preeminent, especially in the field of medical imaging [2].MI has its origins in information theory and exploits the statistical relationship between the source and target images [3, 4]. While it is computationally efficient and robust against outliers, it is sensitive to interpolation artefacts and when the overlap region between images is small. Normalized MI (NMI) [5] was specifically designed to solve this overlap limitation and can successfully align even partial images, provided there is some overlap with the reference image.

One of the challenges for an IR algorithm is the ability to robustly manage differing visual distortions which can occur in a particular domain. Magnetic resonance images (MRI) for example, are prone to non-anatomic intensity variations caused by radio frequency non-uniformities and static field in-homogeneity. This is known as intensity *non-uniformity* (INU), and together with noise, can lead to the corruption of tissue images, which compromises IR quality [6].

A major drawback of both MI and NMI is their failure to accurately register images which contain INU and noise. To resolve this shortcoming, neighbourhood features have been incorporated with MI to secure more robust registration. The effect of INU on IR can be reduced by splitting the image into several regions for feature extraction. Two examples of this approach are gradient MI (GMI) [7] and regional MI (RMI) [8], which combine intensity gradient information and local pixel regions respectively with MI.

To calculate the individual and joint entropies, RMI and its variants [9, 10] use a covariance matrix instead of a high-dimensional histogram to reduce data complexity. However, as a neighbourhood region grows, so does the matrix size, leading to a commensurate computational impact.

The inherent nexus in existing MI techniques between high dimensionality and registration quality provided the motivation to investigate a more efficient MI-based similarity measure for IR, which is both computationally fast and robust to INU and noise. Principal Component Analysis (PCA) [11] is a well-known procedure for reducing data dimensionality and has been integrated with MI (PCA-MI) and used as an IR similarity measure. This feature extraction technique however, requires the whole covariance matrix be computed even if only a few components are desired. This problem is compounded as the matrix dimension increases.

This paper proposes a new MI-based similarity measure which employs *Expectation Maximisation for Principal Component Analysis* (EMPCA) [12] to achieve efficient dimensionality reduction by using an iterative process to determine the dominant principal components. EMPCA-MI uses the first principal component to extract the key features from regions of an image, since this always has the highest variance. This significantly reduces the computational cost, with minimal corresponding impact on the registration performance compared with other MI-based similarity measures. Quantitative results confirm the efficacy of the EMPCA-MI paradigm from both a registration error and computation time perspective on a range of test datasets.

The remainder of the paper is organized as follows: Section 2 briefly reviews the principles of IR, MI and EMPCA, before Section 3 presents the formulation of the EMPCA-MI Model. Section 4 discusses the experimental set-up and a comparative results analysis for the EMPCA-MI. Finally, Section 5 provides some concluding comments.

2. IMAGE REGISTRATION, MI AND EMPCA

A. IR Principles

IR addresses the important task of aligning a source image A with a target image B. This is typically a multistep process [1] which involves: *i)* transforming the coordinates of the source image A in a known reference space; *ii)* generating a new interpolated source image A^* in the reference space; *iii)* comparing A^* with the target image B using a similarity measure; and *iv)* optimizing the transformation parameters to achieve the best possible alignment.

B. MI

MI represents the amount of information one variable contains about another. It assumes a statistical relationship exists between the two variables which is reflected by their individual and joint entropies. For images A and B, their corresponding entropies $H(A)$ and $H(B)$ and their joint entropy $H(A, B)$, are given by:

$$H(A) = -\sum_{a} p_A(a) \log p_A(a) \quad (1)$$

$$H(B) = -\sum_{b} p_B(b) \log p_B(b) \quad (2)$$

$$H(A,B) = -\sum_{a,b} p_{AB}(a,b) \log p_{AB}(a,b) \quad (3)$$

Where a and b are pixel intensities, p_A and p_B denote the individual probabilities of the respective images and p_{AB} is their joint probability. MI is then formally defined as:

$$MI(A,B) = H(A) + H(B) - H(A,B) \quad (4)$$

So MI is maximised when the joint entropy between the images is minimised on a bit-wise pixel basis [3], [4].

C. EMPCA

As mentioned previously, while PCA [11] has been effectively applied to extract features and also formulated with MI (PCA-MI), but similar to RMI, computationally intensive especially as the number of *neighbourhood regions* (NR) increase. This paper uses the EMPCA [12] technique, which is an iterative algorithm to estimate the dominant principal components using an expectation *(e-step)* and subsequent maximisation step *(m-step)*. This has the advantage that it avoids having to compute the entire covariance matrix, which makes EMPCA more efficient. Also since the first dominant principal component has the highest variance for a given NR, it can be used without significantly impacting on the overall IR accuracy. The following section introduces a new EMPCA-MI model formulation, which extracts NR information using EMPCA before applying MI to obtain the statistical relationship between the source and target images.

3. EMPCA-MI MODEL

This paper proposes a fast MI-based similarity measure for IR which is robust to both INU and noise. It combines MI with NR information using EMPCA in three constituent steps. Full details of the EMPCA-MI model are given in Algorithm 1.

Step I: Fig. 1 graphically illustrates this initial step (Lines 1–4 in Algorithm 1), which involves generating the NR matrix **D** for a given pixel radius r. **D** is subsequently concatenated as a 3 dimensional matrix as it scans the whole image, ignoring the margin effects (Lines 2–4). **D** is then reshaped as the NR information matrix Q with dimensions d x N (Fig. 1(b) where d represents the dimensional space and N are total no. of pixels scanned (Line 5). The reason for using NR is to reduce the effect of INU since intensity variations across a localised region will normally be lower than across the whole image. Finally, the information matrix Q is generated for both the target and source images A and B (Line6) as shown in Fig. 1(c).

Step II: Since conventional PCA techniques incur order of $O(Nr^4)$ operations [11], this step is concerned with dimensionality reduction. By applying the iterative EM algorithm, p PCA components [12], where $p<d$, of the largest eigenvectors are determined to decrease the computational overheads. If only the first principal component is considered for example, then the computation complexity incurred is $O(Nr^2)$ in Line 7. While there may be a performance trade-off in terms of the ensuing IR accuracy, as will be evidenced in Section 4, the EMPCA-MI model reduces the overall computational time with only a small impact on registration accuracy compared with other existing MI-based similarity measures.

Step III: The final step evaluates the MI in equation (4) between the first principal components of the target and source images. EMPCA-MI uses the first principal component to extract the features from regions in each image, since it has the highest variance. This represents the dominant features in the images and is used to evaluate the individual and joint entropies in equation (1), (2) and (3). The output of the EMPCA-MI algorithm (Line 8) is a measure of how closely the two images are aligned for the given transformation parameters.

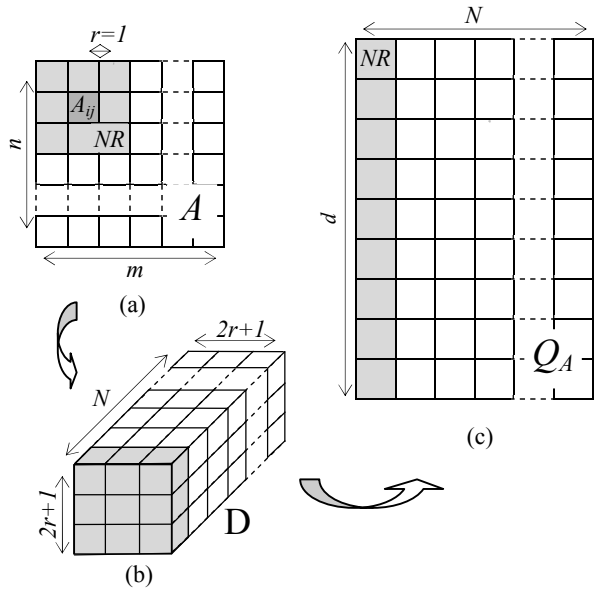

Fig.1 EMPCA-MI Step I illustration (a) source image A with the NR shaded with r=1 from pixel A_{ij}. (b) the corresponding **D** matrix and (c) NR information matrix Q_A

Algorithm 1: EMPCA-MI

Inputs: Images A and B each with spatial resolution m x n *pixels*; r – NR radius.

Variables: d– dimensional space; N– total no. of pixels; *i, j, k*– indexes; **D**–NR square matrix of size $2r+1$; Q_A, Q_B– NR information matrices for A and B; X_A, X_B– first principal component using EMPCA [10] for A and B

Output:EMPCA-MI value

1: Initialise $d = (2r+1)^2$, $N=(m-2r)(n-2r)$ and $k = 1$;
2: For Image A, $1+r \le i \le m-r$, $1+r \le j \le n-r$
3: Define $\mathbf{D}_k=A_{([(i-r)\ldots(i+r)])([(j-r)\ldots(j+r)])}$
4: $k=k+1$
5: Reshape **D** as $Q_{A([1\ldots d])([1\ldots N])}$
6: REPEAT Steps 2 to 5 for Image B to produce Q_B
7: Calculate X_A and X_B using Q_A and Q_B as in [10]
8: Calculate MI(X_A, X_B) using (1),(2),(3) and (4)
9: STOP

. 4. EXPERIMENTAL SETUP AND RESULTS

A series of image registration experiments were undertaken to comparatively analyse the performance of EMPCA-MI algorithm. Four different grayscale image test datasets were used in the experiments to simulate a range of applications and evaluate the robustness of the EMPCA-MI similarity measure to both INU and noise, with the parameter details being provided in Table I. The T1 and T2 MRI image slices were from [13], while the INU function Z [14] was applied to both the *Lena* and *Baboon* images. Gaussian noise was also added to each dataset (see Fig. 2). T1 and T2 images are used to perform multimodal registration. The first series of experiments compared the IR performance of EMPCA-MI with other MI-based similarity measures [3–5] and [7, 8]. To establish the requisite ground-truth, the registration performance was firstly evaluated by mis-registering image B with a known transform.

TABLE I
DATASET PARAMETER DETAILS

Dataset	*Resolution*	*INU*	*Noise(β)*
MRI T1 (T1)	[181 x 217 x 181]	α_{20} = 20% INU, α_{40} = 40% INU	Gaussian (μ = 0.01, σ^2=0.01)
MRI T2 (T2)	[181 x 217 x 181]		
Lena (L)	[256 x 256 pixels]	$Z(x,y)=\frac{1}{3.2}(x+y)^{\dagger}$	
Baboon (Bb)	[256 x 256 pixels]		

$^{\dagger}x$ and y are the spatial coordinates [14].

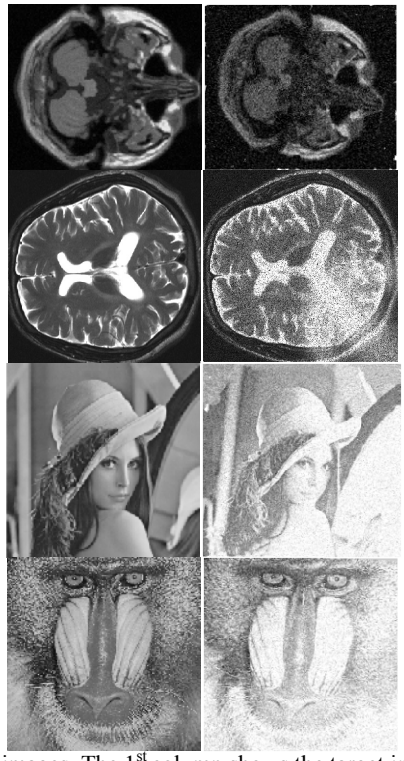

Fig.2 IR test images. The 1st column shows the target images and 2nd column the source images with INU and noise (see Table I).

TABLE II
REGISTRATION ERROR AND AVERAGE RUNTIMES RESULTS

S. No	*A*	*B*	MI[3, 4]	NMI[5]	GMI [7]	RMI [8] (r=1)	EMPCA-MI (r=1)
			ART =0.0762	*ART =0.0943*	*ART =0.1194*	*ART =0.199*	*ART =0.161*
			ΔX, ΔY, Δθ (%)	*ΔX, ΔY, Δθ (%)*	*ΔX, ΔY, Δθ (%)*	*ΔX, ΔY, Δθ (%)*	*ΔX, ΔY, Δθ (%)*
1	T1+α_{20}	T1	9.75, 6.0, 0.56	6.2, 4.0, 0.4	3.0, 2.6, 0.4	5.2, 4.0, 0.44	2.0, 1.3, 0.36
	T1+α_{40}	T1	10.0, 8.3, 0.7	8.5, 6.0, 0.6	5.0, 4.6, 0.46	6.2, 5.3, 0.50	4.5, 4.0, 0.42
	T1+β	T1	11.5, 11.3, 0.78	9.2, 9.3, 0.7	8.0,7.3, 0.5	8.7, 9.3, 0.54	6.0, 7.0, 0.52
	T1+α_{40}+β	T1	13.0, 16.0, 0.9	12.0, 14.6, 0.8	10.0, 10.6, 0.58	10.50, 13.3, 0.62	**8.0, 10.0, 0.58**
2	T1+α_{20}	T2	11.0, 8.3, 0.58	7.5, 7.3, 0.4	4.7, 3.3, 0.5	7.0, 7.0, 0.48	2.6, 2.6, 0.42
	T1+α_{40}	T2	12.0, 9.6, 0.74	9.2, 8.6, 0.6	6.0, 5.6, 0.56	8.0, 9.0, **0.57**	4.8, 4.6, 0.62
	T1+β	T2	13.0, 17.0, 1.2	12.0, 16.0, 1.0	8.7, 8.0, 0.5	11.0, 14.0, 0.52	6.2, 3.0, 0.46
	T1+α_{40}+β	T2	14.5, 19.3, 1.8	13.2, 17.3, 1.4	11.7, 13.6, 0.54	14.0, 19.3, **0.58**	9.7, 4.3, 0.62
3	L+Z	L	0.4, 0.5, 0.24	0.3, 0.4, 0.2	0.27, 0.6, 0.38	0.2, 0.38, 0.21	0.2, 0.32, 0.21
	L+β	L	0.4, 0.6, 0.3	0.3, 0.5, 0.2	0.35, 3.0, 0.43	0.4, 7.00, 0.40	0.32, 0.50, 0.36
	L+*Z*+β	L	14.2, 19.3, 0.42	12.5, 17.0, 0.3	11.0, 21.0, 0.48	9.0, 13.6, 0.24	**2.0, 5.33, 0.21**
4	Bb+Z	Bb	12.7, 3.5, 0.28	6.0, 3.3, 0.2	4.0, 3.3, 0.34	0.6, 1.06, 0.21	0.45, 0.70, 0.21
	Bb+β	Bb	10.7, 5.0, 0.34	5.0, 4.4, 0.2	7.3, 5.2, 0.44	1.4, 20.0, 0.37	0.8, 1.26, 0.21
	*B*b+*Z*+β	Bb	13.5, 17.4, 0.39	12.6, 16.2, 0.3	15.5, 18.0, 0.38	2.0, 2.6, 0.20	**1.4, 1.50, 0.23**

S. No- Scenario Number, *ART*- Average Runtime (*seconds*) and *ΔX, ΔY, Δθ* are percentage registration errors for translations in the X and Y axes and angular rotation respectively.

TABLE III
AVERAGE RUNTIME (SECONDS) FOR SCENARIO 2 REGISTRATION

radius (r)	RMI [5]	PCA-MI	EMPCA-MI
1	0.199	0.912	0.161
3	0.392	1.422	0.386
5	0.904	**4.634**	**0.862**

The registration process involves partial volume interpolation allied with Powell optimisation [2] to estimate the transformation in four separate scenarios (see Table II), representing mono-modal, multi-modal and two generic image registration cases. The mis-registration transformation parameters were all randomly selected from a uniform distribution for the X and Y translations and θ degrees rotation. Table II displays the registration error results for each of the four scenarios in terms of the percentage translation and angular rotational errors. The corresponding average runtimes (ART) for each MI measure are also presented.

The nomenclature in Table II, T1+α_{20} for example, represents MRI T1 image slice with 20% INU, while $L+Z+\beta$ refers to *Lena* having both INU and Gaussian noise artefacts. For both the RMI and EMPCA-MI models, a NR radius of $r=1$ was chosen to investigate the IR performance when a minimal NR is used.

The results confirm that both the RMI and EMPCA-MI similarity measures consistently provide better IR performance in the presence of INU and noise, especially for *Lena* and *Baboon,* at the cost of a small increase in computational time compared with GMI, NMI and MI. Since MI and NMI do not consider spatial features, they are inherently faster but consistently generate larger errors. EMPCA-MI in contrast, provides superior performance in all test scenarios in respect of IR errors as seen in Table II, though RMI produced marginally lower registration error in two occasions in scenario 2 (as highlighted in Table II) of 0.57% and 0.58% when INU and INU together with noise were added respectively. Scenario 2 is a very challenging experiment as the test data (T1 and T2) are multimodals. Generally speaking these results endorse the robustness of the EMPCA-MI measure against both INU and noise as seen in both the mono and multi-modal registrations in scenarios 1 and 2. This also justifies both exploiting NR information and only using the first principal component to improve the computing efficiency by avoiding the calculation of all the eigenvectors.

Another set of experiments were performed to evaluate the EMPCA-MI runtime performance for varying NR radius r, with the corresponding results being shown in Table III for the scenario 2 registration example of T1 MRI with 40% INU and Gaussian noise with T2. While runtime is a resource dependent metric, it offers an insightful comparison between RMI and EMPCA-MI. These experiments also included the conventional PCA-based (PCA-MI) model [11] as a comparator, since this has to generate all the eigenvectors. As expected, the ART increase commensurately with r since more neighbourhood regions are incorporated into the d space, though EMPCA-MI again provided a lower ART of 0.862*secs* compared with 4.634*secs* for PCA-MI. The reason for this discrepancy is that PCA-MI as mentioned above has to generate all components from the covariance matrix before selecting the dominant ones. Interestingly, as the resolution of the test images is increased, it is observed this computation becomes a NP-complete problem for PCA-MI.

5. CONCLUSION

This paper has presented a new MI-based similarity measure which applies *Expectation Maximisation for Principal Component Analysis* (EMPCA-MI) to achieve more robust image registration performance and enhanced computational efficiency. The EMPCA-MI model reduces the latent dimensionality problem in other MI-based solutions, while concomitantly providing comparable registration performance, particularly in the presence of intensity non- uniformity and noise artefacts.

6. REFERENCES

[1] B. Zitova "Image registration methods: A survey", *Image Vision Computer*, vol. 21(11), pp.977-1000, 2003.

[2] J. P. W. Pluim , J. B. A Maintz and M. A. Viergever "Mutual-information-based registration of medical images: A survey", *IEEE Trans. Med. Imag.,* vol. 22(8), pp. 986-1004, 2003.

[3] P. Viola and W. M. Wells III, "Alignment by maximization of mutual information", Proc. 5th Int. Conf Computer Vision, pp.16-23, 1995.

[4] Collignon, F. Maes, D. Delaere, D. Vandermeulen, P. Suetens, and G. Marchal, "Automated multi-modality image registration based on information theory," Imaging, vol. 3(1), pp. 263-274, 1995.

[5] C. Studholme, D.L.G.Hill and D.J. Hawkes, "An Overlap Invariant Entropy Measure of 3D Medical Image Alignment", Pattern Recognition, Vol. 32(1), pp 71-86, 1999.

[6] A. Simmons, P. S. Tofts, G. J. Barker, and S. R. Arridge, "Sources ofintensity nonuniformity in spin echo images at 1.5 T," *Magn.Reson.Med.*, vol. 32, pp. 121–128, 1994.

[7] J. P. Pluim, J. B. Maintz, and M. A. Viergever, "Image registration by maximization of combined mutual information and gradient information," *IEEE Trans. Med. Imag.*, vol. 19(8), pp. 809-814, 2000.

[8] D. B. Russakoff, C. Tomasi, T. Rohlfing et al, "Image similarity using mutual information of regions." in ECCV (3), pp. 596-607, 2004.

[9] C. Yang, T. Jiang, J. Wang, and L. Zheng, "A Neighborhood Incorporated Method in Image Registration," Image Rochester NY, pp. 244-251, 2006.

[10] P. A. Legg, P. L. Rosin, D. Marshall, and J. E. Morgan, "A robust solution to multi-modal image registration by combining mutual information with multi-scale derivatives.," Medical Image Computing and Computer-Assisted Intervention, vol. 12(1), pp. 616-623, 2009.

[11] I. Jolliffe, Principal Component Analysis, 2nd ed. New York: Springer, 2002.

[12] S. Roweis, "EM algorithms for PCA and SPCA," in Advances in Neural Information Processing Systems, 10, 1998.

[13] D.L. Collins, A.P. Zijdenbos, V. Kollokian, J.G. Sled, N.J. Kabani, C.J. Holmes, A.C. Evans : "Design and Construction of a Realistic Digital Brain Phantom" *IEEE Trans. Med. Imag*., vol.17(3), p.463–468, 1998.

[14] J. D. Garcia-Arteaga and J. Kybic, "Regional image similarity criteria based on the Kozachenko-Leonenko entropy estimator."In CVPRW (8), pp. 1-8, 2008.